Peroxide mediated metal oxide nanoparticle synthesis via hydrolysis under mild conditions.

Brian Neltner[*] William Doenlen[†] Scott Speakman[‡]
Angela Belcher[§]

November 3, 2009

Abstract

A wide variety of metal oxide nanoparticles were synthesized using hydrogen peroxide as an etchant to prevent particle growth during hydrolysis under basic conditions, starting from a metal chloride precursor in aqueous solution. XRD is used to show that increased amounts of hydrogen peroxide cause a decrease in particle size. In many cases, the metal oxide was formed immediately with a nanocrystallite size ranging from 1 nm to several tens of nanometers. After synthesis, the particles were dried and heat treated to investigate phase changes and particle growth after calcination.

1 Introduction

Metal oxides represent a very large class of materials useful in a variety of applications including electronics, optics, ceramics, and catalysts.[1] Many applications that are dependent upon the surface area of the material or size of the crystallite domain can be further enhanced through the use of the nanoparticle form of metal

[*]Department of Materials Science and Engineering, Massachusetts Institute of Technology, Cambridge
[†]Department of Materials Science and Engineering, Massachusetts Institute of Technology, Cambridge
[‡]Department of Materials Science and Engineering, Massachusetts Institute of Technology, Cambridge
[§]Department of Materials Science and Engineering & Department of Bioengineering, Massachusetts Institute of Technology, Cambridge, E-mail: belcher@mit.edu

oxides.[2] As such, metal oxide nanoparticles have garnered much research interest over the past few decades, both in novel applications and new synthesis methods.

Current metal oxide nanoparticle synthesis methods represent an eclectic ensemble of chemical processes; many, however, produce fairly large crystallite domains, require toxic chemicals, or take place only under extreme conditions whereas our new method produces small crystallites, uses benign precursors, and takes place at room temperature. Organometallic methods and microemulsion methods have also been used to synthesize metal oxide nanoparticles under mild conditions.[3–5] A number of methods also use either aqueous or organic solvents, with or without the use of a surfactant, and generally take place under mild conditions.[2,6,7] However, few of these syntheses apply to a wide range of materials, have very small crystallite sizes, and the use of surfactants or microemulsions can impact the purity and accessibility of crystallite faces in the final materials.

Methods that require more extreme conditions include spray pyrolysis, hydrogen-plasma metal reactions and hydrothermal reactions at supercritical conditions.[8–11] None of the above methods, however, have been reported to synthesize a broad class of metal oxide nanoparticles of very small nanocrystallite size, and instead appear to be used only in the synthesis of a small number of metal oxides. A key to any new synthesis methods for mixed phase nanocrystalline materials, and a useful starting point for potentially making complex single-phase ceramics, is that the materials can be made using compatible synthesis techniques, so a synthesis which is able to be used to make a wide variety of materials is critical.

2 Results and discussion

The 22 different materials formed with this synthesis were categorized into a number of groups. Of the materials attempted, 15 of them appeared to readily form either the oxide or a mostly amorphous material which appeared to be oxide and which transformed into identifiable oxide after a heat treatment at 400°C for 2 hours. Four more materials formed a non-oxide phase initially, but were transformed into the oxide after heat treatment at 400°C for 2 hours.

Each of the samples was analyzed using XRD as initially prepared and after heat treatment in order to get an estimate of crystallite size. In the case of the

Precursor	Init Prod	Init Size	400°C Prod	400°C Size
$CeCl_3$	CeO_2	3.0	CeO_2	5.0
$CoCl_3$	Co_3O_4	4.5	Co_3O_4	6.9
$DyCl_3$	Dy_2O_3	1.1	Dy_2O_3	1.3
$ErCl_3$	Er_2O_3	1.0	Er_2O_3	1.3
$GdCl_3$	Gd_2O_3	1.1	Gd_2O_3	1.3
$InCl_3$	In_2O_3	<1	In_2O_3	1.2
$LuCl_3$	Lu_2O_3	1.0	Lu_2O_3	1.1
$MnCl_2$	Mn_3O_4	13.2	Mn_3O_4	15.5
$RhCl_3$	Rh_2O_3	<1	Rh_2O_3	4.0
$RuCl_3$	RuO_2	2.9	RuO_2	34.6
$SmCl_3$	Sm_2O_3	3.8	Sm_2O_3	5.0
$SnCl_3$	SnO_2	<1	SnO_2	1.2
$TbCl_3$	Tb_2O_3	1.0	Tb_4O_7	1.4
YCl_3	Y_2O_3	1.0	Y_2O_3	1.0
$YbCl_3$	Yb_2O_3	1.0	Yb_2O_3	1.3

Table 1: Fifteen of the materials attempted with this synthesis method were made easily and appeared to immediately form the oxide with no heat treatment. In each case, the sample was heat treated, and the nanocrystallite size as measured by XRD peak broadening was recorded, with the assumption that all samples are nanocrystalline. In the case of terbium oxide, the oxide changed color, which we infer indicated a phase transformation from Tb_2O_3 to Tb_4O_7 based on the reported colors of the respective oxides. Nanocrystallite sizes are reported in nanometers.

samples which were consistent with either a nanocrystalline or an amorphous interpretation, the size was determined from the peak broadening of the lower angle peak only, to remove errors which would be introduced by incorrectly fitting the amorphous part of the spectra to nanocrystalline peaks.

In each case, the initially formed oxide, initial nanocrystallite size, final oxide formed, and final nanocrystalline size are reported. In some cases, the specific oxide phases are uncertain, and in these cases our best guess as to the phase of the materials is given. In most systems, the XRD is consistent with a highly nanocrystalline material, but some materials may instead be amorphous. The materials which were readily synthesized in this way are listed in Table 1.

In most cases, the initially formed nanoparticles are exceptionally small, with an estimated particle size of approximately 1 nm or less for 9 of the samples. The only sample which began with a crystallite size greater than 4.5 nm was Mn_3O_4, showing the general advantage gained by using peroxide to inhibit particle growth and encourage the formation of only very small nanocrystals. In many cases, there was very little crystallite growth during the heat treatment phase, although in the

Precursor	Init Prod	400°C Prod	400°C Size
$CuCl_2$	$Cu(OH)_2$	CuO	22.7
$FeCl_3$	Hematite+FeO(OH)	Hematite	1.4/amorph
$NiCl_2$	$Ni(OH)_2$	NiO	9.6
$ZnCl_2$	Mixed	ZnO	16.3

Table 2: The materials which initially formed a non-oxide phase in a large amount, but which fully transformed to the oxide phase upon heat treatment at 400°C for 2 hours. The initially formed phase, final phase, and final phase nanocrystallite size estimate in nanometers are shown. Mineral names are given where a chemical formula does not fully specify the phase.

case of RuO_2 there was a very significant size increase.

In the case of four of the attempted materials, the initially formed phase was not the oxide, but after heat treatment at 400°C, the material transformed fully into the oxide as listed in Table 2. In three of these cases, the initial material was the related hydroxide, but in the case of zinc oxide, the initially formed material had a large number of unidentifiable phases present. However, all of the unidentifiable phases disappeared upon heat treatment.

Representative XRD spectra and corresponding TEM micrographs for cobalt oxide and lutetium oxide, which appeared to be definitively crystalline, are shown in Fig. 1. XRD and TEM for terbium oxide and iron oxide, which are not obviously crystalline, are shown in Fig. 2.

Ceria (CeO_2) was used as a typical metal oxide for investigating the effect of hydrogen peroxide concentration on particle size. At a H_2O_2:Metal ratio of 0.0580:1 the particle sizes were approximately 6.5 nm. At a ratio of 58.0:1, the size decreases to approximately 2.3 nm. Sizes were verified with TEM analysis on images with $\sim$100 nanocrystallites visible, and the size was fit to a log-log plot which gave a fit of

$$d = 3.93 \cdot C^{-0.16}$$

using the TEM data, and

$$d = 3.70 \cdot C^{-0.18}$$

using the data from XRD, showing good agreement. The XRD patterns for the ceria samples taken at various peroxide concentrations, as well as the log-log fit across the range of concentrations are shown in Fig. 3 along with representative TEM. From the figure showing the fit, it can be seen that the agreement diverges for

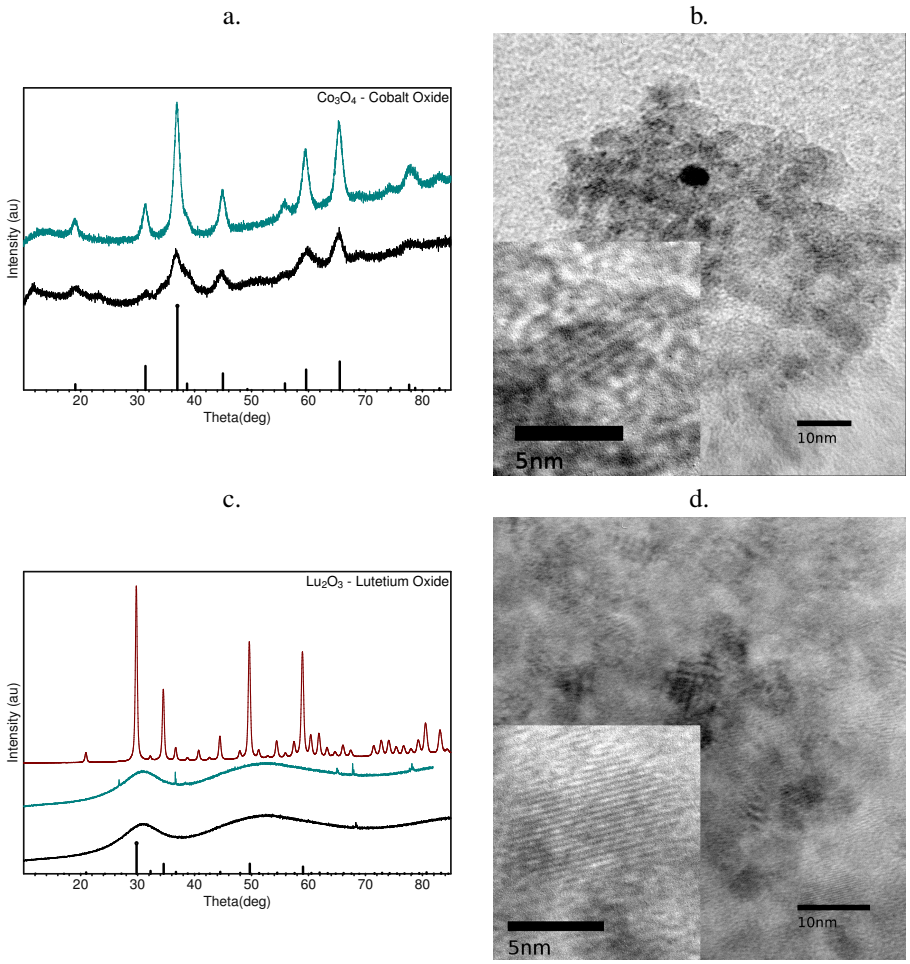

Figure 1: XRD patterns of definitely crystalline nanoparticle samples. In each case, the bottom XRD pattern corresponds to the "as prepared" sample, the next to a 400°C sintered sample, and the next, if present, is an 800°C sintered sample. Each XRD pattern is shown with lines associated with the phase it was identified as. TEM is shown of the "as prepared" sample with inserts having a scalebar of 5 nm and the main image having a scalebar of 10 nm (a) Cobalt oxide XRD. (b) Cobalt oxide TEM with insert showing lattice fringes. (c) Lutetium oxide XRD. (d) Lutetium oxide TEM with insert showing crystallinity.

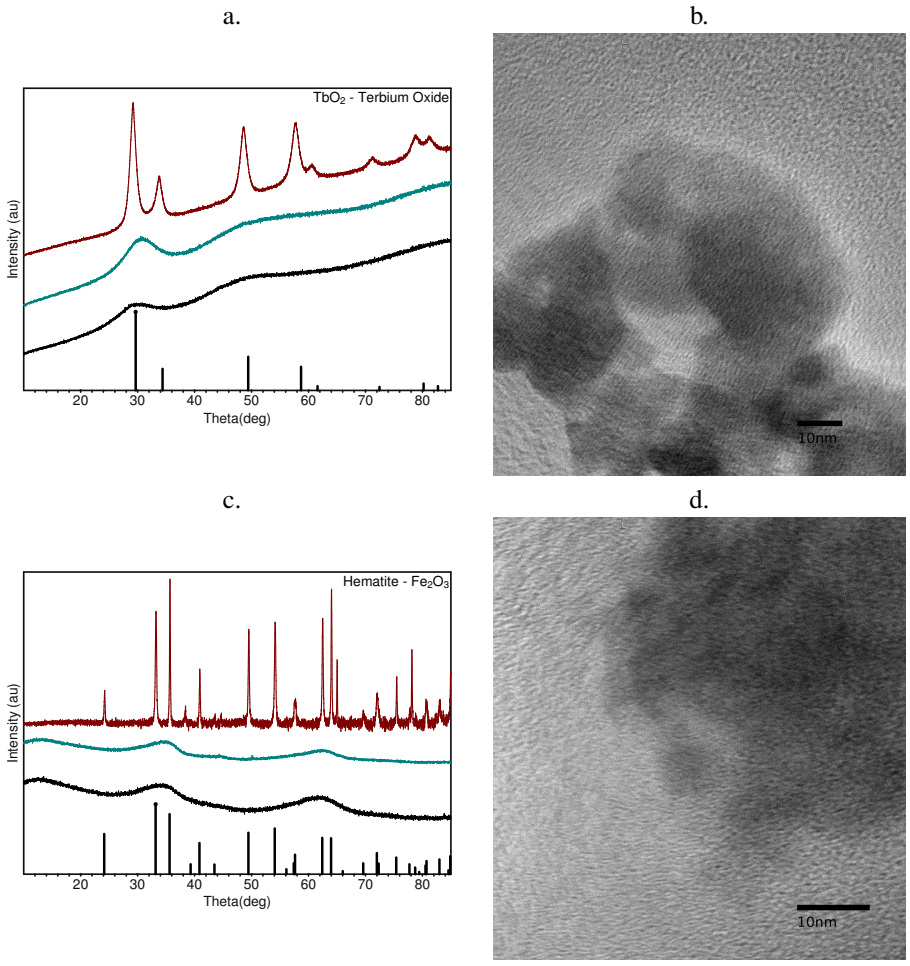

Figure 2: XRD patterns of nanoparticle samples with no clear initial crystallinity. In each case, the bottom XRD pattern corresponds to the "as prepared" sample, the next to a 400°C sintered sample, and the next, if present, is an 800°C sintered sample. Each XRD pattern is shown with lines associated with the phase it was identified as. TEM is shown of the "as prepared" sample with 10 nm scalebars in each image. (a) Terbium oxide XRD. (b) Terbium oxide TEM. (c) Iron oxide XRD. (d) Iron Oxide TEM.

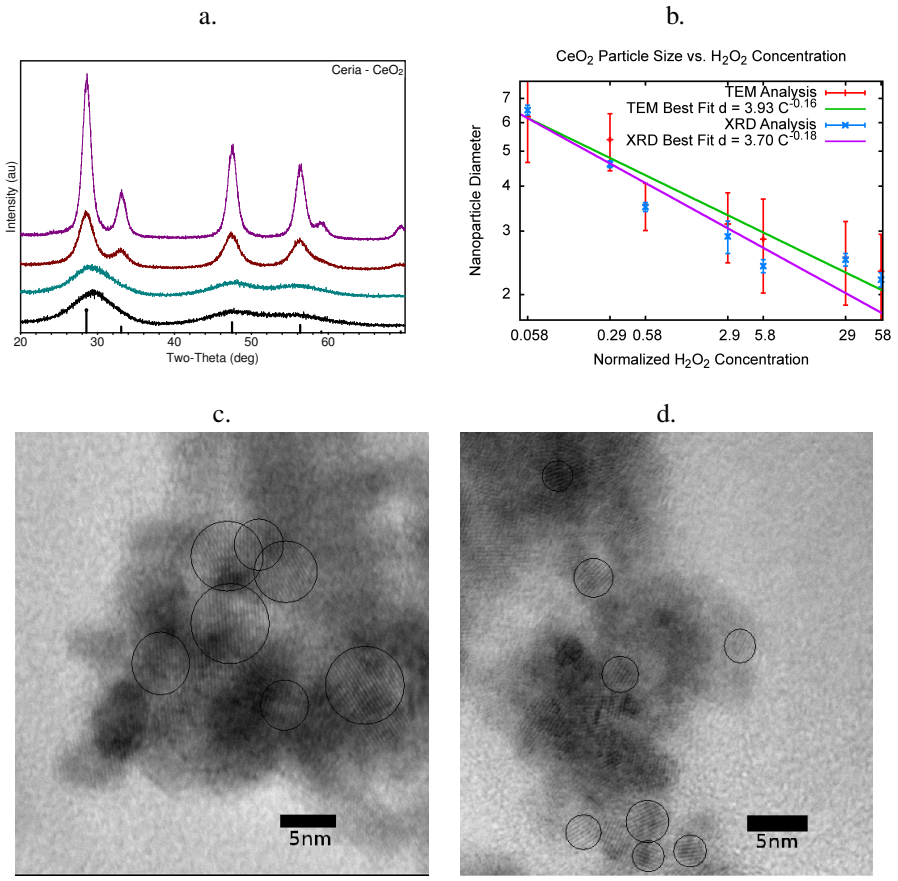

Figure 3: A demonstration of size control using CeO_2 as a typical metal oxide system. (a) XRD spectra of CeO_2 synthesized using 0.058:1, 0.58:1, 5.8:1, and 58:1 H_2O_2:Metal ratios from top to bottom, showing the clear decrease in particle size as peroxide concentration increases. Data at 5.8:1 and 58:1 are essentially overlapping. (b-c) TEM of CeO_2 made at a 0.058:1 ratio (b) and 58:1 ratio (c) of peroxide to metal with single crystalline domains highlighted.

small particle sizes, which is expected due to the difficulty in using XRD to make accurate measurements for crystallite sizes below 5 nm, as well as the difficulty in imaging lattice fringes for extremely small crystalline particles. For very large concentrations of hydrogen peroxide, the reaction was exothermic, and caused rapid evolution of gas. Special care was taken with a secondary containment vessel in case the flask overflowed. However, after a few minutes, the reaction equilibrated and stabilized.

Further, Co_3O_4 was used to show the oxidation process in more detail. In this case, XRD data shown in Fig. 4 shows how at extremely low concentrations of hy-

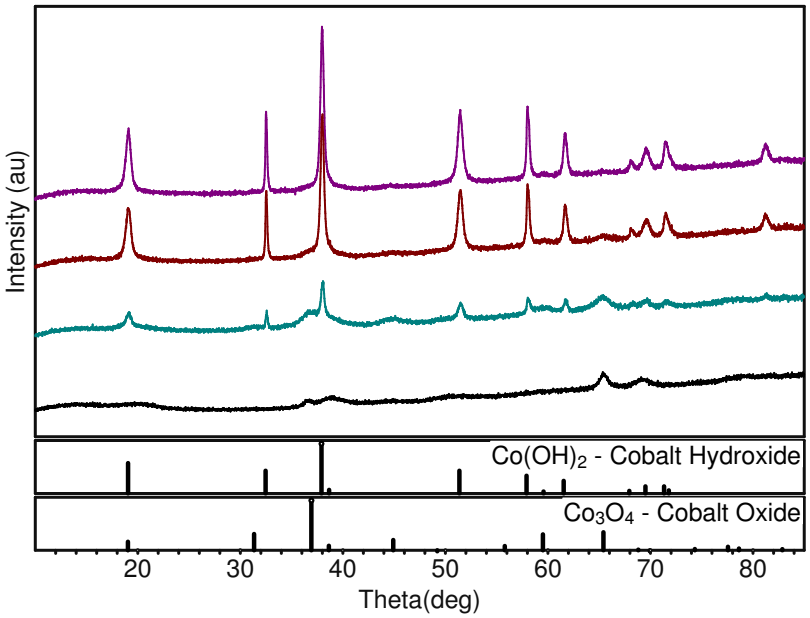

Figure 4: A demonstration of the oxidation process in Co_3O_4 showing increasing amounts of added hydrogen peroxide. As hydrogen peroxide is added in higher concentrations, the amount of $Co(OH)_2$ decreases, and the amount of Co_3O_4 increases. The ratio of H_2O_2:Metal in the top set of data is 0.00232:1, and moving down the graph the ratios are 0.0232:1, 0.232:1, and 2.32:1.

drogen peroxide, 0.00232:1 (1x), the material is entirely $Co(OH)_2$ of a fairly large particle size, showing that the hydroxide can easily form large particles. However, as the hydrogen peroxide concentration is increased up to a ratio of 2.32:1 (1000x), the hydroxide disappears and is replaced by extremely small Co_3O_4 particles, although the size of the accompanying $Co(OH)_2$ particles does not change much. This series of XRD patterns is consistent with hydrolysis to small soluble hydroxide materials in basic solution due to the presence of NaOH, followed by oxidation when hydrogen peroxide is present, or to larger hydroxide particles when hydrogen peroxide is not present.

Three of the materials we attempted to synthesize did not form an oxide even upon heat treatment at 400°C (Table 3). In the case of lanthanum oxide, it formed instead lanthanum hydroxide $La(OH)_3$ of fairly large particle size. The lanthanum hydroxide particles appear to shrink upon heat treatment, suggesting that they are being gradually converted into another material, and indeed the amorphous back-

Precursor	Init Prod	800°C Prod
$LaCl_3$	$La(OH)_3$	La_2O_3+LaOCl
$NdCl_3$	$Nd(OH)_3$+NdOCl+amorph	Nd_2O_3+NdOCl
$PrCl_3$	$Pr(OH)_3$	PrO_2

Table 3: The materials which did not convert to an oxide readily after a 400°C heat treatment for 2 hours are shown. In each case, after further heat treatment at 800°C, the material formed the oxide as a majority phase, and in some cases also contained a chloride impurity.

ground appears to increase in the heat treated sample. However, after heat treating the sample at 800°C, the majority of the sample is in the La_2O_3 or the LaOCl phase with a small impurity of $La(OH)_3$, suggesting that this material simply requires a higher temperature for full conversion. The chloride is likely a residual of using a chloride precursor, and switching to a nitrate precursor should remove this byproduct.

In the case of neodymium oxide, the initial synthesis produced a combination of large $Nd(OH)_3$ and NdOCl particles with a background of about 1 nm particles of an unidentifiable phase. The unidentifiable phase represented approximately 60% of the spectrum. After heat treatment at 400°C, the amorphous background grew to the dominant phase, and is clearly not $Nd(OH)_3$ or NdOCl. Upon heat treatment at 800°C, it becomes clear that the other phases were being converted into Nd_2O_3, and almost all of the peaks present are Nd_2O_3. However, there is a small impurity of NdOCl, likely possible because of the presence of chloride precursor. If it was desired to remove the chloride, it should be possible to do the same synthesis with nitrate precursors.

The praseodymium oxide synthesis initially formed a material readily identifiable as praseodymium hydroxide $Pr(OH)_3$. Upon heat treatment, the color changed from a pale green to brown, and the XRD became a more complicated mixed phase of $Pr(OH)_3$ and PrO_2. The amount of PrO_2 was small compared to the $Pr(OH)_3$ amount, but appeared to be increasing as the sample was heated for longer times.

In terms of trends, the three most difficult materials are all located near each other on the periodic table and would have formed a 3^+ oxide. Cerium, the element between them, formed the 4^+ oxide immediately upon synthesis, suggesting that if the lanthanum, praseodymium, and neodymium had a stable 4^+ oxide, they may have been able to form readily.

The four materials which formed the oxide after a mild heat treatment were also all very close to each other on the periodic table, and several began as the 2^+ salt. The remaining materials all formed an extremely small oxide readily and rapidly at room temperature with no heat treatment.

3 Experimental

Using a method derived from that developed by Yamashita *et al*,[12] nanocrystals of various metal oxides were formed using precipitation via hydrolysis in aqueous solution of a corresponding metal chloride or metal chloride hydrate by adding NaOH and H_2O_2. Yamashita *et al* used 45.1 mmol of H_2O_2 with 100 mmol of metal precursor, giving a molar ratio of 0.451:1 (H_2O_2:Metal) based on the measured value of the density of 6 wt% H_2O_2 being 1.02 gm/mL.

To produce nanoparticle powders for testing, 100 mL of 100 mM metal chloride solution is stirred rapidly in a 250mL Erlenmeyer flask for 30 minutes. Next, 200 uL of 30 wt% H_2O_2 is added to 10 mL of 3 M NaOH solution in a separate flask, and the mixed NaOH/H_2O_2 solution is added rapidly to the metal chloride solution. In typical experiments, there is an immediate color change, followed by gradual equilibration over 30 minutes. The supernatant is removed by centrifugation, precipitate is washed with millipore water to remove any remaining NaCl, and centrifuged again. This is repeated for a total of three washings. Finally, the supernatant is discarded and precipitate is dried in air at room temperature.

The amount of hydrogen peroxide used represents 2.32 mmol based on the measured density of 30 wt% H_2O_2 of 1.31 gm/mL, so with 10 mmol of metal precursor, the ratio of hydrogen peroxide to metal in the synthesis is 0.232:1.

After synthesis, the dried precipitate is split into two samples of roughly equal size. One is heat treated at 400°C for 2hr. Both samples are analyzed with XRD, and several samples were also analyzed with TEM to give an idea of the nanostructure of the produced materials.

4 Summary

We have demonstrated an extremely simple method for producing very small nanocrystals of a very wide range of metal oxides in aqueous solution using only mild precursors. The technique was also used to control the size of ceria nanoparticles by using varying concentrations of hydrogen peroxide, and was shown to be able to control the ratio of cobalt hydroxide and cobalt oxide formed via hydrolysis by using small amounts of hydrogen peroxide.

This technique is primarily novel in the use of extremely high concentrations of hydrogen peroxide as a surface etchant to acheive size control, as well as applying this general oxidation method to a wide collection of materials known to be amenable to hydrolysis. We suspect that the peroxide forms defects on the surface of forming nanocrystals, inhibiting particle growth while allowing or even encouraging particle nucleation in cases where oxidation is a fast process compared to hydrolysis. The result is substantially improved kinetics towards producing extremely small nanoparticles. In cases where hydrolysis is faster than oxidation due to either thermodynamic driving forces or due to concentrations of peroxide, hydroxide may instead be formed first, and only later be broken up into small oxide particles.

Due to the wide range of nanoparticles synthesized using the same method, it is also very likely that the reported syntheses can be mixed to great effect in order to produce highly nanocrystalline mixed material systems. Further, the materials reported in this work also represent a good starting set of compounds for future attempts at synthesizing complex single-phase ceramics.

References

[1] K. F. C. Bluthardt, C. Fink, *Catalysis Today*, 2008, **137**, 132–143.

[2] G. Oskam, *J Sol-Gel Sci Techn*, 2006, **37**, 161–164.

[3] B. Chaudret, *C.R. Physique*, 2005, **6**, 117–131.

[4] G. G. M. Niederberger, *Chem. Eur. J.*, 2006, **12**, 7282–7302.

[5] S. V. A. Ganguli, T. Ahmad, *Pure Appl. Chem.*, 2008, **80**, 2451–2477.

[6] C. C. J. Jolivet, S. Cassaignon, *J Sol-Gel Sci Technol*, 2008, **46**, 299–305.

[7] Z. J. I. Djerdj, D. Arcon, *Journal of Solid State Chemistry*, 2008, **181**, 1571–1581.

[8] H. Y. K. D. Y. Kim, S. H. Ju, *Journal of Alloys and Compounds*, 2006, **417**, 254–258.

[9] H. S. U. J. H. Kim, Y. C. Hong, *Surface & Coatings Technology*, 2007, **201**, 5114–5120.

[10] H. S. T. Liu, Y. Zhang, *Langmuir*, 2003, **19**, 7569–7572.

[11] K. S. T. Adschiri, Y. Hakuta, *Journal of Nanoparticle Research*, 2001, **3**, 227–235.

[12] Y. F. M. Yamashita, S. Yoshida, *Journal of Materials Science*, 2001, **37**, 683–687.